

## CHAPTER 125

### A QUASI-3D MATHEMATICAL MODEL OF COASTAL MORPHOLOGY

H.J. de Vriend<sup>\*)</sup> and J.S. Ribberink<sup>\*)</sup>

#### ABSTRACT

A semi-analytical model of 3D nearshore currents and sediment transport is presented. It describes the tidal motion, the waves, the surfzone currents and the sediment transport in complex coastal areas. The results of a first application, to a well-documented case at the Dutch coast, indicate the potential and the shortcomings of the model. The latter are analysed and suggestions for improvement are given.

#### INTRODUCTION

Mathematical models are increasingly important as a tool to predict the water and sediment motion in coastal areas. Still, most of these models consider only part of the sediment transport. Roughly speaking, they describe either the "longshore" or the "cross-shore" transport. More carefully formulated, they consider either the transport along with the time- and depth-averaged current, or the transport due to waves and vertical circulations (undertow) in a more or less cross-shore profile. In complex situations, this distinction makes little sense and neither transport component can be disregarded. In these situations, the 3D time-dependent flow field and the attending sediment motion have to be described (cf. De Vriend, 1986).

In view of the wide range of time scales involved, from some seconds for the wind waves through to half a day for the tide, fully-3D time-dependent simulations are hardly feasible for practical applications. Therefore, simplified models have to be used, taking due account of the relevant phenomena.

De Vriend and Stive (1987) propose a semi-analytical model of 3D nearshore currents, based on hydrostaticity and similarity hypotheses for the velocity components and the eddy viscosity. This so-called DVS-model, in a slightly modified form, is combined here with a sediment transport model based on the Bagnold-Bailard concept (Bailard, 1981), to yield a quasi-3D coastal transport model.

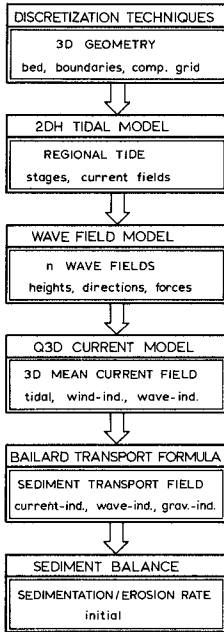
After a brief description of this model, a first practical application, with both "longshore" and "cross-shore" transport mechanisms at work, is described and discussed. It concerns the rapid formation of large sand bank systems on the former ebb-tidal deltas of the estuaries closed off by the Deltaworks (Kohsiek, 1988). The results are compared with field data, and the model formulation is reconsidered.

#### GENERAL OUTLINE OF THE MODEL

The model consists of the following basic elements (see Figure 1).

- A regional tidal model, giving the tidal stages and the boundary conditions for the flow model in the area of interest. The velocity field

<sup>\*)</sup> Senior researcher, DELFT HYDRAULICS, P.O. Box 152, 8300 AD EMMELOORD, The Netherlands



from this model can be used in the wave model, in order to have a rough indication of the effects of current refraction.

- A wave field model, describing the propagation and dissipation of wind waves in the area of interest.
- A quasi-3D current model, describing the wave orbital motion and the mean flow due to tide and wave action.
- A Bailard-type sediment transport formula, describing the near-bed transport due to waves (stirring, asymmetry transport) and currents ("convective" transport).
- The sediment balance equation, yielding the sedimentation/erosion rate under the given conditions.

These elements are put in line, as indicated in Figure 1, without any feedback mechanisms. This means that detailed current refraction, for instance, is disregarded, and that the dynamic interaction between the water and sediment motion and the bed topography changes are left out of consideration.

Figure 1 Aggregate flow chart of the quasi-3D morphological model

## CURRENT MODEL

### Primary and secondary flow

Key elements in the quasi-3D current model (De Vriend and Stive, 1987) are similarity approximations for the eddy viscosity,  $\nu_t$ , and the wave-averaged velocity,  $\bar{U}$ :

$$\nu_t(x, y, z; t) = \bar{\nu}_t(x, y; t) \phi(\zeta) \quad (1)$$

$$\bar{U}(x, y, z; t) = \bar{U}(x, z; t) f_p(\zeta) + \sum_k \bar{U}_k(x, z; t) f_k(\zeta) \quad (2)$$

in which:  $x, y$  = horizontal co-ordinates,  
 $z$  = vertical co-ordinate,  
 $t$  = time,  
 $\zeta = \frac{z - z_b}{h}$  = boundary-fitted vertical coordinate,  
 $z_b$  = bottom level,  
 $h$  = water depth, and  
 $\bar{\cdot}$  = depth-average.

The first product in the RHS of (2) is called the "primary flow velocity". The vertical distribution function  $f_p(\zeta)$  is chosen the same as in uniform shear flow under the same conditions (turbulence, waves, bed roughness, etc.). Hence the primary flow accounts for the (as yet unknown) depth-averaged velocity as if it concerned uniform shear flow. The remaining part of the wave-mean velocity is called "secondary flow velocity", although this name is disputable. It is supposed to consist of a number of constituents, for each of which vertical similarity is assumed. In the present version of the model the secondary flow concerns

wave-induced undertow and boundary layer streaming, but there is no reason why it should be restricted to these phenomena.

In addition to the wave-mean velocity, there is an oscillatory velocity associated with the waves. For the time being, these velocities are simply added together, although in reality they are interacting (Davies et al., 1988; Klopman and De Vriend, 1988).

#### Depth-averaged current model

The depth-averaged mean velocity,  $\vec{U}$ , is computed with a horizontally two-dimensional shallow water model, including the effects of wind, tide and short waves. The latter exert their influence through the forcing, the bottom shear stress relationship and the mass balance (mass flux compensation). The wave influence on the horizontal eddy viscosity (Wind and Vreugdenhil, 1986; Yoo and O'Connor, 1988) is left out of consideration, as the model is meant for rather large-scale problems (model extension  $\gg$  surf zone width) with irregular waves.

The system of differential equations solved by the model can be written as

$$\frac{D\vec{U}}{Dt} = -g \vec{\nabla}(z_s) - \frac{\vec{\tau}_b}{\rho h} + \frac{\vec{F}_w}{\rho h} + \nu_h \vec{\nabla} \cdot \vec{\nabla}(\vec{U}) \quad (3)$$

$$\frac{\partial z_s}{\partial t} + \vec{\nabla} \cdot (h\vec{U}) + \vec{\nabla} \cdot \left(\frac{\vec{M}}{\rho}\right) = 0 \quad (4)$$

in which:  $g$  = acceleration due to gravity,  
 $z_s$  = level of the mean water surface,  
 $\rho$  = mass density of the fluid,  
 $\vec{\tau}_b$  = bottom shear stress,  
 $\vec{F}_w$  = external driving force (wind, waves),  
 $\nu_h$  = horizontal eddy viscosity, and  
 $\vec{M}$  = wave-induced mass flux.

Note that this system differs from the one in the DVS-model, in that the mass flux compensation is treated as a part of the primary flow, rather than as a secondary flow constituent. Thus the mass flux compensation can take place through a horizontal circulation or a circulation in the vertical plane, depending on the geometrical situation. Besides, it is continuous in the horizontal plane, now, so that the attending bed shear stresses and sediment transports are more smoothly distributed in space.

The wave-induced forces and mass fluxes can be derived explicitly from the wave model, as they depend on wave field properties only. The following formulations are used in the DVS-model

$$\vec{F}_w = \frac{D}{\omega} \vec{k}_w \quad (5)$$

$$\vec{M} = (1 + 7 \tilde{Q}_b \frac{h}{\lambda}) \frac{E}{\omega} \vec{k}_w \quad (6)$$

in which:  $D$  = energy dissipation rate per unit area,  
 $E$  = energy density of the wave field,  
 $\omega$  = angular frequency of the waves,  
 $\vec{k}_w$  = wave number, as a vector in the direction of the wave energy flux,  
 $\tilde{Q}_b$  = fraction of the waves that is breaking ( $0 \leq \tilde{Q}_b \leq 1$ ), and  
 $\lambda$  = wave length.

The bottom shear stress consists of two parts, due to the primary and the secondary flow, respectively. In the DVS-model, the secondary shear stress is supposed to be negligible in the depth-averaged flow computation. The primary shear stress depends on the current velocity and on the waves, so it cannot be computed on the basis of wave data only. In order to close the mathematical system (3) through (6), this shear stress has to be expressed in terms of the depth-averaged velocity.

In the present version of the depth-averaged current model, Bijker's (1966) shear stress enhancement formula is used, in the approximative form

$$\frac{\vec{\tau}_b}{\rho} = C_f \vec{U} |\vec{U}| \left[ 0.75 + 0.45 \left( \xi \frac{\hat{U}_{orb}}{|\vec{U}|} \right)^{1.13} \right] \geq C_f \vec{U} |\vec{U}| \quad (7)$$

in which:  $C_f$  = bottom friction factor for current only,

$$\xi = (f_w)^{\frac{1}{2}} (2C_f)^{-\frac{1}{2}},$$

$f_w$  = Jonsson's (1966) friction factor for waves, and

$\hat{U}_{orb}$  = amplitude of the near-bottom orbital velocity.

Following Visser's (1986) suggestion, the factor  $\xi$  is taken identically equal to 1. The orbital velocity in this expression is calculated as if it concerned regular and linear waves, with the mean amplitude and the peak period of the actual random wave field.

The shear stress relationship is closely connected with the turbulence model (vertical eddy viscosity, bottom boundary condition), and hence with the description of the primary velocity profile. In this respect, relationship (7) is not consistent with the original DVS-model (cf. Ribberink and De Vriend, 1988). Since the bed shear stress is the only aspect of the primary flow that is used in the sediment transport model, this inconsistency is not expected to have serious consequences for the model.

### Primary flow profile

Consistently with the similarity assumption for the primary flow, the vertical profile function  $f_p(\zeta)$  is solved from the horizontal momentum equation for uniform shear flow, rewritten to

$$\frac{\partial}{\partial \zeta} \left( \epsilon \frac{\partial f}{\partial \zeta} \right) = C_\tau \quad \text{with} \quad C_\tau \hat{=} \frac{|\vec{\tau}_{bp}| h}{\rho \bar{v}_c |\vec{U}|} \quad (8)$$

in which  $\vec{\tau}_{bp}$  denotes the primary bottom shear stress.

With the parabolic/constant eddy viscosity distribution of the DVS-model and a prescribed level of zero-intersection of the (logarithmic) profile near the bottom, this leads to

$$f_p(\zeta) = \begin{cases} -\frac{3}{1+3 \ln(2F'\zeta_0)} \{ \ln \zeta - \ln(F'\zeta_0) \} & \text{for } F\zeta_0 \leq \zeta \leq \frac{1}{2} \\ \frac{3}{1+3 \ln(2F'\zeta_0)} \left\{ -2\zeta^2 + 4\zeta - \frac{3}{2} - \ln(2F'\zeta_0) \right\} & \text{for } \frac{1}{2} \leq \zeta \leq 1 \end{cases} \quad (9)$$

in which:  $\zeta_0$  = the level of zero-intersection for currents alone,

$F'$  = amplification factor for the wave influence on the level of zero-intersection, and

$F\zeta_0$  = lowest level at which the logarithmic velocity profile holds good.

In the DVS-model, the amplification factor  $F'$  and  $F$  are formulated as proposed by Nielsen (1985). It is also possible, however, to choose a formulation that corresponds with (7):

$$F' = \exp \left[ \kappa C_F^{-\frac{1}{2}} \left( 1 - X_p^{-\frac{1}{2}} \right) \right] \quad (10)$$

in which  $\kappa$  denotes Von Karman's constant and  $X_p$  is defined by

$$X_p = \min \left\{ 1, 0.75 + 0.45 \left( \frac{\hat{U}_{orb}}{|\bar{U}|} \right) \right\} \quad (11)$$

Once  $F'$  is known,  $F$  follows from the same relationship as in Nielsen's model, viz.

$$F' = F \exp \left[ \frac{1}{F} - 1 \right] \quad \text{and hence } F \approx eF' - 1 \quad (12)$$

in which  $e$  denotes the neperian.

### Secondary flow

So far, the model has been elaborated for secondary flow due to wave breaking and for the residual streaming in the oscillatory boundary layer at the bottom.

Exploratory computations (De Vriend and Stive, 1987; Stive and De Vriend, 1987) indicate that the latter component is of minor importance to the short-term residual sediment transport. Therefore, only the breaking-induced secondary flow will be considered. The DVS-model uses the effective surface shear stress

$$\bar{\tau}_t = \left( \frac{1}{2} + 7 \frac{h}{\lambda} \right) \frac{D}{\omega} \bar{k}_w \quad (13)$$

to drive this part of the current, assuming  $\bar{\tau}_t$  to act at the wave trough level,  $\tau = \tau_t$ . The corresponding secondary velocity can be written as

$$\bar{U}_1 = \bar{U}_{1,1} f_{s1}(\tau) + \bar{U}_{1,2} f_{s2}(\tau) \quad (14)$$

$$\text{with: } \bar{U}_{1,1} = \frac{\bar{\tau}_t h}{\rho \bar{v}_t \tau_t} \quad \text{and} \quad \bar{U}_{1,2} = \frac{\bar{\tau}_{bs} h}{\rho \bar{v}_t \tau_t} \quad (15)$$

Here  $\bar{\tau}_{bs}$  denotes the secondary part of the bottom shear stress, directed along the vertical plane through the wave rays and as yet unknown in magnitude. The vertical distribution functions are those given by De Vriend and Stive (1987), which means that  $f_{s1}(\tau)$  represents the velocity profile due to a surface shear stress and  $f_{s2}(\tau)$  closely resembles the normal shear flow profile.

The magnitude of  $\bar{\tau}_{bs}$  follows from the requirement that the depth-averaged secondary flow velocity must be zero. Hence

$$|\bar{\tau}_{bs}| = - \frac{\overline{f_{s1}} |\bar{\tau}_t|}{\overline{f_{s2}}} = - \left( \frac{1}{2} + 7 \frac{h}{\lambda} \right) \frac{\overline{f_{s1}} D}{\overline{f_{s2}} \omega} |\bar{k}_w| \quad (16)$$

$$\text{in which: } \overline{f_{s1}} = \frac{25}{144} \quad (17)$$

$$\overline{f_{s2}} = -\frac{25}{144} - \frac{5}{48} \tau_t \{-1 + 2 \ln(2F' \tau_o)\} \quad (18)$$

Note that the secondary flow is not the same as the flow due to the surface stress  $\tau_t$ . The latter obviously has an  $f_{s1}$ -type profile. As  $\overline{f_{s1}}$  is non-zero, however, the present framework of definitions, which forms the basis of the quasi-3D model, makes it necessary to split this flow into a primary and a secondary part, as shown in Figure 2. The secondary part is given by (14) sqq., the primary part is included in the primary flow model, with a minor inconsistency because  $f_p(\zeta)$  and  $f_{s2}(\zeta)$  are not exactly identical.

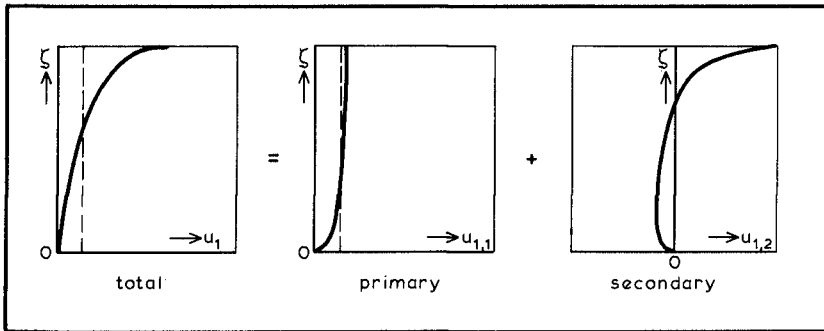


Figure 2 Splitting of the flow due to a surface shear stress

This primary flow contribution is driven by part of the wave-induced force  $\overline{F}_w$  in (3). This means that there is no guarantee for this contribution to be actually present. Depending on the geometrical situation, the relevant force field can just as well generate a water level set-up, or a current in a different direction, or any combination of these. Hence the interpretation of 3D currents due to breaking waves as a superposition of a longshore current with the primary profile and a cross-shore current (undertow) with the secondary profile (Svendsen and Lorenz, 1988) is only valid for very specific situations. In more general cases, a wide range of vectorial combinations of primary and secondary flow components can be found, and the notions "longshore" and "cross-shore" make no sense for such currents.

## SEDIMENT TRANSPORT MODEL

### Basic concept

A sediment transport model for coastal areas should include what uses to be called "longshore" and "cross-shore" transport components. In view of the discussion in the previous section, this should rather be "convective" and "wave-asymmetry" transport components.

Most of the usual coastal transport models pertain to the convective transport, with the wave-mean current as a transporting agent and wave action as one of the stirring mechanisms.

Such models are expected to fail in the complex situations considered herein.

On the other hand, the mechanisms underlying what is summarized by the term "wave-asymmetry" transport, such as vortex shedding at rippled beds

(Nielsen, 1988) and sheet-flow over a plane bed (Bakker and Van Kesteren, 1988), are far from being fully understood, let alone that well-established models would be available.

A pragmatic way-out is to adopt a sediment transport formula that is claimed to describe the instantaneous transport rate, and formally integrate the result over the waves. This approach was followed by e.g. Madsen and Grant (1976) and Bailard (1981). The latter adopted Bagnold's (1966) energetics approach and worked it out for colinear waves and currents. Although this model concept is still subject to doubt and will not apply to every possible set of conditions (cf. De Waal, 1987; Nielsen, 1988), it has yielded quite acceptable results in large-scale laboratory tests (Roelvink and Stive, 1988) and in practical applications (Stive, 1986). Therefore, it is incorporated in the present morphological model system, at least for the time being.

The transport formulae forming the Bailard-model, generalized to any vectorial combination of waves and currents, can be written as

$$\vec{q}_{bed} = A_{bc} \langle |\vec{U}_t|^2 \vec{U}_t \rangle - A_{bs} \langle |\vec{U}_t|^3 \rangle \vec{v}(z_b) \quad (19)$$

$$\vec{q}_{sus} = A_{sc} \langle |\vec{U}_t|^3 \vec{U}_t \rangle - A_{ss} \langle |\vec{U}_t|^5 \rangle \vec{v}(z_b) \quad (20)$$

in which:  $\vec{q}_{bed}$  = bed load transport rate,  
 $\vec{q}_{sus}$  = suspended-load transport rate,  
 $\vec{U}_t$  = equivalent instantaneous near-bed velocity,  
 $A_{..}$  = factors depending on the sediment properties, etc., and  
 $\langle .. \rangle$  = wave-average of the argument.

Note that this model includes both bed load and suspended-load transport. Besides, the down-slope gravitational transport component is taken into account in the bed load part. The bottom slope term in the suspended-load part represents the effect of convection by the slope-induced vertical velocity component.

#### Instantaneous near-bed velocity

The equivalent near-bed velocity,  $\vec{U}_t$ , in (19) and (20) remains to be specified. Following Bailard (1981), it consists of a mean and an oscillatory component. So, in a generalized form, this reads

$$\vec{U}_t = \vec{U}_o + \vec{U}_w \quad (21)$$

The definition of the mean flow part,  $\vec{U}_o$ , is not obvious, in view of the steep velocity gradients near the bottom. Bagnold's (1966) model was derived for steady uniform flow with a depth-invariant velocity and the usual quadratic friction law. Taking the bottom shear stress as determinative for the transport, the equivalent velocity can be expressed by

$$U_o = \left( \frac{\tau_b}{\rho C_f} \right)^{\frac{1}{2}} \quad (22)$$

or, in a generalized form for more complex steady flows,

$$\vec{U}_o = \frac{\vec{\tau}_b}{\rho C_f^{\frac{1}{2}} |\vec{U}_*|} \quad \text{with} \quad |\vec{U}_*| = \left( \frac{|\vec{\tau}_b|}{\rho} \right)^{\frac{1}{2}} \quad (23)$$

The oscillatory component of the equivalent near-bed velocity,  $\vec{U}_w$ , is filled in with the near-bed orbital velocity of waves in an inviscid fluid, as if there were no current and no bottom boundary layer. This is consistent with Bailard's (1981) approach.

Since wave-asymmetry is an important agent in wave-induced sediment transport, linear wave theory is not sufficient here. Instead, the orbital velocity is described with Rienecker and Fenton's (1981) Fourier-approximation technique for non-linear waves. Although the underlying theory is formally restricted to steady progressive waves on a horizontal bottom, the technique is applied throughout the wave field. Rienecker and Fenton showed this to be allowable for non-breaking waves, but the applicability to breaking waves is disputable. By lack of a good ready-to-use alternative, however, this point is ignored for the time being.

#### Elaboration of the time-mean transport

The formal algebraic elaboration of the generalized Bailard-formula, i.e. substitution of (21) into (19) and (20) and averaging over the wave period, becomes fairly complicated (cf. Guza and Thornton, 1985). Therefore, it was decided to evaluate the transport numerically in every point of the computational grid and at every time step of the computation. This turned out not to lead to prohibitive computer expenses.

#### VOORDELTA: A FIRST APPLICATION

##### Situation

The closure, as part of the Deltaworks, of several estuaries in the South-west of The Netherlands has started off a spectacular morphological evolution of the former ebb-tidal deltas (see, for instance, Kohsiek, 1988). After the in- and outgoing tide had been blocked, the dynamic equilibrium between the cross-shore actions of waves and currents was disturbed and the waves started pushing the seaward edges of the deltas onshore.

Within a decade, huge sand bank systems were formed in front of the barriers (Figure 3; also see: Van der Spek, 1987; Van den Berg, 1987), which raised questions about their future development and their impact on the coastal defence system, the local ecosystem, the possibilities of economical use, etcetera. Therefore, the Ministry of Public Works (Rijkswaterstaat) and DELFT HYDRAULICS are executing extensive studies in this area.

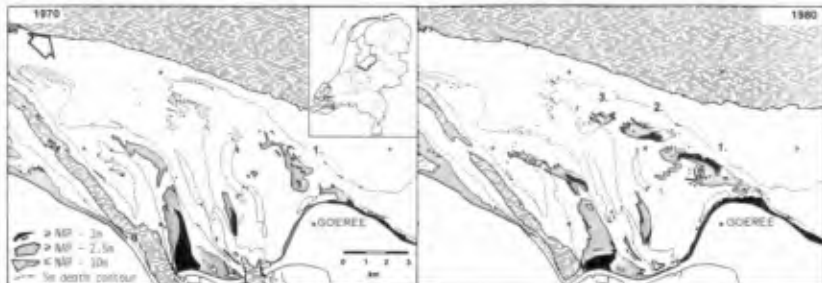


Figure 3 Deformation of the ebb-tidal delta in the mouth of the Grevelingen estuary, after closure of the Brouwersdam (from: Van der Spek, 1987)

As far as morphology is concerned, these studies are aiming at a better understanding and a hindcast of the observed phenomena, and at the prediction of future morphological developments.

As a part of these studies, a first practical application of the present model system was to hindcast and predict the morphological evolution of the ebb-tidal delta in front of the Brouwersdam, in the former mouth of the Grevelingen estuary (Figure 3).

#### Results of previous studies in the area

A preliminary hindcast study with a numerical model of coastal profile evolution (Stive, 1986; see Figure 4) indicated that the onshore transport due to wave asymmetry must be an important agent in the formation of the sand banks, with the offshore transport due to undertow and gravitational effects as a principal counteracting agent.

Further study of bathymetric and sedimentological data, and an extensive hindcast study with the coastal profile model (Steetzel and Stive, 1986) made clear, that the morphological processes in the later stages of development are essentially 3D, with an interaction between tidal and wave-induced currents. The following phenomena were expected to be important:

- "vertical" tide, with flooding and drying of sand banks and, correspondingly, time-varying wave penetration into the area behind the banks,
- tidal currents,
- wave-induced undertow,
- sediment stirring by waves, and
- wave-asymmetry transport.

A quasi-3D sediment transport model was set up in order to see how the combination of these phenomena works out, and as a tool in overall hindcast and forecast studies, for the Grevelingen delta as well as the adjacent Haringvliet and Eastern Scheldt deltas.

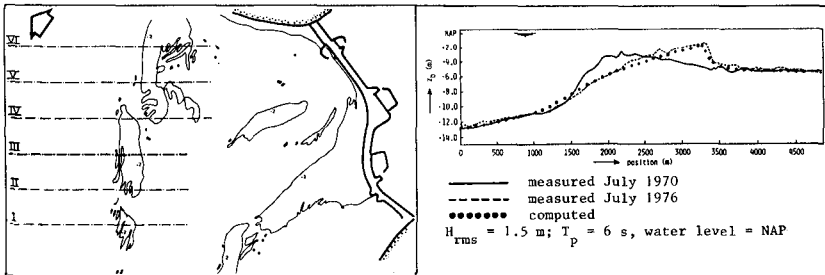
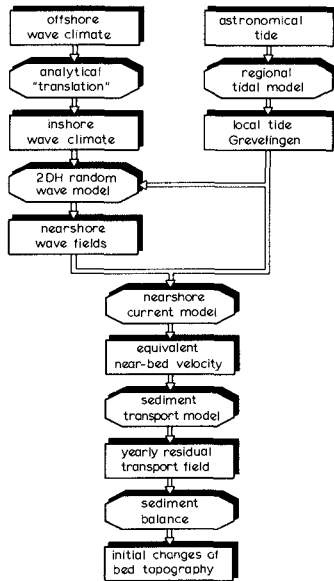


Figure 4 Results of hindcast with cross-shore profile model (from: Stive, 1986)

#### Set-up of the quasi-3D model for the Grevelingen delta

The composition of the quasi-3D model for the Grevelingen-area is outlined in Figure 5. The principal constituents are

- the regional tidal model RANDELTA-II (Langerak et al., 1978), based on the WAQUA-code and developed and validated to support the Deltaworks; this model is used to generate the tidal stages and a rough estimate of the current field to be put into the wave computations, and the tidal boundary conditions for the detailed current model,
- a series of wave models, one for each incoming wave direction, based on the HISWA-code (Holthuysen and Booij, 1986; Dingemans, 1987), which takes randomness of wave height and direction into account,
- a depth-integrated detailed current model for combined tidal and wave-induced currents, based on the curvilinear version of the WAQUA-code (Willemse et al., 1985), extended with wave effects as described in the foregoing (also see: De Vriend and Van Banning, 1988),



- the semi-analytical bottom shear stress model, including 3D flow effects, as described in the foregoing,
- the generalized Bailard transport formula, and
- a sediment balance module, yielding the initial rate of sedimentation and erosion for a given transport field.

Feedback mechanisms (wave-current interaction, topography-hydrodynamics interaction) are not included, for technical as well as economical reasons. This implies that the model results remain to be interpreted in terms of longer-term morphological evolutions.

The model constituents work on different types of grids and cover different areas, having the area of interest in common. This implies that a number of interfaces is needed to transform model results from one grid to another.

Figure 5 Flow chart Grevelingen model

The constituents, together with their interfaces and pre- and postprocessing facilities were brought together into an envelope system taking care of data management, job control, etcetera (cf. Boer et al., 1984). This made it possible to handle the large number of runs needed to represent the net effects of natural variability.

### Schematization

Morphological changes, as a longer-term process, reflect the net effects of tide and wave climate, including their natural short-term variability. The model should therefore take this variability into account.

Since the system is multi-dimensional, complicated, and non-linear, spectral approaches and linear systems theory are likely to fail. Also a representative combination of tidal and wave conditions, yielding after e.g. one year the same morphological changes as the natural conditions, is hard to find, if it exists, at all. Therefore, a pragmatic schematization procedure was followed here (Van Banning and De Vriend, 1987; Steijn, 1988).

Key elements in this procedure are the selection of a morphologically equivalent tidal cycle and the schematization of the wave climate. The criterion for the tidal cycle selection is that the yearly transport rate, according to a given transport formula (in this case: Van Rijn's (1986) formula) should be the same for the repeated equivalent cycle and for the actual astronomical tide. In principle, this can yield a different equivalent cycle in every point of the model area. Therefore, a limited number of representative points was chosen, and the cycle with the best overall fit was selected.

The wave climate was schematized in three steps, viz.

- three representative wave directions (approximately NW, W and SW) were chosen on the basis of the available wave data,
- for each directional class, a representative wave height was chosen,
- each directional class, and the situation without waves, were attributed a certain weight, such that the weighed model results can be expected to represent the yearly transports and sedimentation/erosion rates.

Two criteria were used to determine these weights for the convective transport. The "longshore power" criterion (SPM, 1984) was used to account for the convective transport in the surf zone. The second criterion concerns the correct representation of the "stirring parameter", defined as the ratio between the primary bottom shear stress with and without waves. If this criterion is satisfied, the model is supposed to reproduce the convective transport outside the surfzone.

As the wave-asymmetry transport varies with a much higher power of the wave height than the convective transport, different weight factors were applied for this transport component. The criterion was a correct reproduction of the transport according to the Bailard formula without mean currents.

Like in the tidal schematization, full agreement can only be required in a small number of representative points.

### Validation

A compound model like this is usually validated by checking the results of its principal constituents individually, and those of the model as a whole, against measured data, general observations, logical expectations, etcetera.

The available tidal data (water levels, current velocities) from the Grevelingen area were sufficient to check the detailed current model in situations without significant waves (Van der Spek and Steijn, 1988). Wave-driven current data, however, were not available in an identifiable form, so that earlier field and laboratory verifications (De Vriend and Van Banning, 1988) had to be relied upon.

Wave data from the area of interest are hardly available, but the wave model concept has been verified in the adjacent Haringvliet area (Holt-huijsen et al., 1988).

Sediment transport data are lacking, too, but the available sedimentological data (Van der Spek, 1987; Van den Berg, 1987) give some insight into the net displacement of sediment. Besides, the successful hindcast with the coastal profile model (Stive, 1986) gives confidence in the Bailard-formula.

In order to check the model as a whole, the morphological evolution of the area between the closure of the dam (1971) and 1984 was hindcasted and compared with bathymetric and sedimentological data. The outcome of this comparison will be discussed in the next sections.

## ANALYSIS OF HINDCAST RESULTS

### Results of the 2DH model version

In order to have a reference and a back-up for the quasi-3D model, a parallel run was made with a two-dimensional horizontal (2DH) version of the model, in which no secondary bottom shear stress was incorporated in the transport model. The results, shown in Figure 6, look rather satisfactory. Although the sediment transport rate is somewhat too high all over the area, the general picture from Figure 3 is represented: the bars tend to move onshore and towards the tip of the northern island, and a second array of bars tends to form half-way the first one and the dam. Besides, though not visible in the plots, the aggradation of the area behind the outer bars is reproduced.

### Results of the quasi-3D model version

The results of the full quasi-3D model, including the secondary shear stress in the transport model, are shown in Figure 7. Even though the quasi-3D model takes more of the physical phenomena (viz. undertow) into

account than the 2DH model, its results are far worse: the bars are even moving seawards now!

This unexpected result needs further analysis. If the present case allows for a 2DH approach, the additional effects introduced by the quasi-3D model must be unimportant and should therefore do no harm. The present results show otherwise, which suggests that the quasi-3D model still contains a major inconsistency.

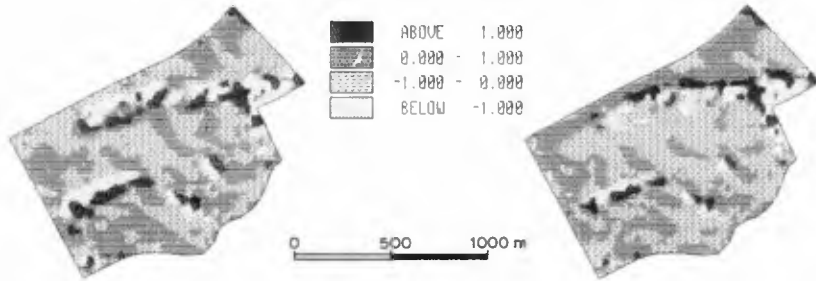


Figure 6 Sedimentation/erosion rate (2DH model version)

Figure 7 Sedimentation/erosion rate (quasi-3D model version)

#### Analysis and discussion

As was stated before, the hindcast studies with the cross-shore profile model indicated that the onshore wave-asymmetry transport should be the principal bank generating agent here, with the transport due to undertow and downslope gravitational effects as a counteracting agent. When introducing a net current across the bank, however, the undertow turned out to be easily dominated (Steetzel and Stive, 1986). According to the results of the 2DH detailed current model, such across-bank currents are present, indeed.

- The (NE-going) flood current is trapped between the coastline and the outer bank array and gives rise to a strong offshore current across the banks. The (SW-going) ebb current, however, more or less follows the alignment of the bank array, which is partly dry by that time. Hence the residual tidal current on the banks is directed offshore.
- Especially for waves from NW and W, the banks act more or less as an underwater bar, attached to Goeree at the one end and ending in the open sea at the other. This situation, which is very similar to the wave tank experiment reported by Dingemans et al. (1986), gives rise to a wave-induced horizontal circulation that is directed onshore on the top of the banks and directed towards the open-sea end in the channel behind them.

The velocities due to either of these currents dominate the undertow velocity. This suggests the bank formation to be due not only to wave-asymmetry transport, but also to the wave-induced horizontal circulation, with the residual tidal current as the principal counteracting agent. Besides, if the net effect is neatly reproduced by a cross-shore profile model containing much weaker currents only, the effects of the two currents must be almost balancing. This means that a relatively weak disturbance of this balance, e.g. by introducing 3D-effects in an inconsistent manner, can have strong effects.

Since the only difference between the 2DH and quasi-3D versions of the model lies in the secondary bottom shear stress, the quasi-3D model must be inconsistent in its incorporation of this stress. Upon closer inspec-

tion, the trouble must be caused by disregarding  $\tau_{bs}^+$  in the depth-averaged flow equations (3). This can be illustrated by considering the strongly simplified one-dimensional momentum equation

$$0 = -g \frac{\partial z}{\partial x} - \frac{\tau_{bx}}{\rho h} + \frac{F_{wx}}{\rho h} \quad (24)$$

in which the x-axis is directed onshore, perpendicular to the bank crest. Depending on the geometrical situation, the wave-induced force  $F_{wx}$  will contribute to sustaining a current or a set-up of the water level. In the Grevelingen area, with the wide channel behind the banks, only little set-up will build up. In that case, equation (24) reduces to

$$\tau_{bx} = F_{wx} \quad (25)$$

If the secondary shear stress is disregarded, like in the present model,

$$\tau_{bpx} = F_{wx} \quad (25)$$

In the sediment transport model, however,  $\tau_{bs}$  is added to  $\tau_{bp}$ , so

$$\tau_{bx} = \tau_{bpx} + \tau_{bsx} = F_{wx} + \tau_{bsx} \quad (26)$$

Since, according to (16),  $\tau_{bsx}$  is negative (directed offshore; also see Figure 2), the onshore convective transport is systematically underestimated. This explains why the quasi-3D model predicts an offshore movement of the banks. It also explains why the 2DH-model works well in this particular situation with little set-up: the correct value of  $\tau_{bx}$  is  $F_{wx}$ , and hence  $\tau_{bpx}$ ! Although the 2DH model suffices for the Grevelingen area, this will not be so for all practical situations: set-up and undertow are not always negligible. Therefore, the inconsistency in the quasi-3D model has to be removed. The remedy is simple and straightforward: include  $\tau_{bs}^+$  in the depth-averaged current model.

## CONCLUSIONS

A quasi-3D model of the yearly residual sediment transport and bed topography changes in complex coastal areas was applied to a practical situation, where previous studies had indicated that 3D effects (undertow) should be important.

In this particular case, however, a depth-integrated version of the model, without 3D effects, turned out to give a good hindcast of the observed morphological evolutions, in spite of remaining doubts about the transport model.

A comparison with the much worse results of the quasi-3D model provided the possibility to trace a major inconsistency in the latter: the secondary bottom shear stress should not be disregarded in the depth-averaged current model, if it is taken into account in the sediment transport model. Once this inconsistency has been removed, the model can be a useful tool for the analysis of morphological processes in complex coastal areas.

## ACKNOWLEDGEMENT

The development of a pilot version of the model, as well as its application to the Grevelingen area, were performed by order of the Ministry of

Transport and Public Works (Rijkswaterstaat), by a joint project-team of this organization and DELFT HYDRAULICS. The authors are members of this team.

#### REFERENCES

- Bagnold, R.A., 1966. An approach to the sediment transport problem from general physics. USGS Prof. Paper, 422-1.
- Bailard, J.A., 1981. An energetics total load sediment transport model for a plane sloping beach. *J. Geoph. Res.*, **86**, C11, p. 10938-10954.
- Bakker, W.T. and Van Kesteren, W.G.M., 1986. The dynamics of oscillating sheetflow. Proc. 20th ICCE, Taipei, p. 940-954.
- Bijker, E.W., 1966. The increase of bed shear in a current due to wave action. Proc. 10th ICCE, Tokyo, p. 746-765.
- Boer, S., de Vriend, H.J. and Wind, H.G., 1984. A mathematical model for the simulation of morphological processes in the coastal area. Proc. 19th ICCE, Houston, p. 1437-1453.
- Davies, A.G., Soulsby, R.L. and King, H.L., 1988. A numerical model of the combined wave and current bottom boundary layer. *J. Geoph. Res.*, **93**, no. C1, p. 491-508.
- De Vriend, H.J., 1986. 2DH computations of transient sea bed evolutions. Proc. 20th ICCE, Taipei, p. 1698-1712.
- De Vriend, H.J. and Stive, M.J.F., 1987. Quasi-3D modelling of nearshore currents. *Coastal Engineering*, **11**, no. 5/6, p. 565-601.
- De Vriend, H.J. and Van Banning, 1988. Depth-averaged tidal and wave-induced current modelling for application in the Voordelta area of the Dutch coast. DELFT HYDRAULICS, Rept. H526-3 (in preparation).
- De Waal, J.C.M., 1987. Investigation on Bailard's transport formula, applied to cross-shore transport. Delft University of Technology, Dept. of Civil Engrg., M.Sc. thesis (in dutch).
- Dingemans, M.W., 1987. HISWA verification in the directional wave basin. DELFT HYDRAULICS, Rept. H228-1.
- Dingemans, M.W., Stive, M.J.F., Bosma, J., de Vriend, H.J., Vogel, J.A., 1986. Directional nearshore wave propagation and induced currents. Proc. 20th ICCE, Taipei, p. 1092-1106.
- Guza, R.T. and Thornton, E.B., 1985. Velocity moments in the nearshore. *J. Waterway, Port, Coastal and Ocean Engrg.*, **111**, no. 2, p. 235-256.
- Holthuijsen, L.B. and Booij, N., 1986. A grid model for shallow water waves. Proc. 20th ICCE, Taipei, p. 261-270.
- Holthuijsen, L.B., Booij, N. and Herbers, T.H.C., A prediction model for stationary short-crested waves in shallow water with ambient currents. To be published in *Coastal Engineering*.
- Jonsson, I.G., 1966. Wave boundary layers and friction factors. Proc. 10th ICCE, Tokyo, p. 127-148.
- Klopman, G. and De Vriend, H.J., 1988. Modelling of velocity profiles due to waves and currents in the coastal zone. Proc. 21st ICCE, Malaga.
- Kohsiek, L., 1987. Reworking of former ebb-tidal deltas into large long-shore bars following the artificial closure of tidal inlets in the southwest of The Netherlands. In: P.L. de Boer et al. (eds.) "Tide-influenced sedimentary environments and facies". Reidel Publ. Comp., Dordrecht.
- Langerak, A., de Ras, M.A.M. and Leendertse, J.J., 1978. Adjustment and verification of the Randdelta II model. Proc. 16th ICCE, Hamburg, p. 1049-1070.
- Madsen, O.S. and Grant, W.D., 1976. Sediment transport in the coastal environment. Mass. Inst. Techn., R.M. Parsons Lab., Rept. no. 209.
- Nielsen, P., 1985. A short manual of coastal bottom boundary layers and sediment transport. Public Works Dept. N.S. Wales, Coastal Engrg. Branch, Rept. TM 85/1.

- Nielsen, P., 1988. Three simple models of wave sediment transport. Coastal Engineering, 12, no. 1, p. 43-62.
- Ribberink, J.S. and De Vriend, H.J., 1988. Sediment transport formulations for waves and currents in the Voordelta area of the Dutch coast. DELFT HYDRAULICS, H526-2 (in preparation).
- Rienecker, M.M. and Fenton, J.D., 1981. A Fourier approximation method for steady waves. J. Fluid Mech., 104, p. 119-137.
- Roelvink, J.A. and Stive, M.J.F., 1988. Large scale tests of cross-shore sediment transport on the upper shoreface. Proc. IAHR-Symp. Sed. Transp. Coastal Zone, Copenhagen, p. 137-147.
- Shore Protection Manual, 1984. US Army Corps of Engineers, Waterways Exp. Station, Vicksburg.
- Stetzel, H.J. and Stive, M.J.F., 1986. Cross-shore transport study Voordelta. Delft Hydraulics Laboratory, Report H239 (in dutch).
- Steyn, R.C., 1988. Schematization of the natural conditions in multi-dimensional numerical models of coastal morphology. DELFT HYDRAULICS, Rept. H526-1 (in preparation).
- Stive, M.J.F., 1986. A model for cross-shore sediment transport. Proc. 20th ICCE, Taipei, p. 1551-1564.
- Stive, M.J.F. and De Vriend, H.J., 1987. Quasi-3D nearshore current modelling: wave-induced secondary current. Proc. ASCE Spec. Conf. "Coastal Hydrodynamics", Delaware p. 356-370.
- Svendsen, I.A. and Lorenz, R.S., 1988. Three dimensional flow profiles on littoral beaches. Proc. 21st ICCE, Malaga.
- Van Banning, G.K.F.M., de Vriend, H.J. and Boer, S., 1987. Schematization and validation of 2DH mathematical models in coastal morphology. Proc. "Coastal Sediments '87" Conf., New Orleans, p. 600-615.
- Van den Berg, J.H., 1987. Note on the isallobath map Voordelta 1975-1984. Rijkswaterstaat, Directorate Zeeland, Rept. ZL 87.0020 (in dutch).
- Van der Spek, A.J.F., 1987. Description of the development of the outer deltas of Haringvliet and Grevelingen. Rijkswaterstaat, Dept. Tidal Waters, Rept. GWA0-87-015 (in dutch).
- Van der Spek, A.J.F. and Steijn, R.C., 1988. Confrontation of mathematical model results and measured data for the Grevelingen outer delta. Rijkswaterstaat, Dept. Tidal Waters, Rept. GWA0-88.1320 (in prep.).
- Van Rijn, L.C., 1986. Three-dimensional modelling of suspended sediment transport for currents and waves. DELFT HYDRAULICS, Rept. H461/Q250/Q422.
- Visser, P.J., 1986. Wave basin experiments on bottom friction due to current and waves. Proc. 20th ICCE, Taipei, p. 807-821.
- Willemsse, J.B.T.M., Stelling, G.S. and Verboom, G.K., 1986. Solving the shallow water equations with an orthogonal coordinate transformation. Int. Symp. Comp. Fluid Dyn., Tokyo (also: DELFT HYDRAULICS Comm. 356).
- Wind, H.G. and Vreugdenhil, C.B., 1986. Rip-current generation near structures. J. Fluid Mech., 171, p. 459-476.
- Yoo, D. and O'Connor, B.A., 1988. Turbulence transport modelling of wave-induced currents. Proc. Int. Conf. Comp. Mod. Ocean Engrg., Venice, p. 151-158 (Balkema, Rotterdam, 1988).